Available online at www.sciencedirect.com

SCIENCE DIRECT

Materials Letters 59 (2005) 2468 – 2471

materials letters

www.elsevier.com/locate/matlet

Poly(methyl methacrylate) monolayers at the air–water interface

I. Çapan[a], R. Çapan[a,*], T. Tanrisever[b], S. Can[b]

[a]Balikesir Üniversitesi Fen-Edebiyat Fakültesi Fizik Bölümü Balikesir 10100 Turkey
[b]Balikesir Üniversitesi Fen-Edebiyat Fakültesi Kimya Bölümü Balikesir 10100 Turkey

Received 10 February 2005; accepted 20 March 2005
Available online 21 April 2005

Abstract

Several poly(methyl methacrylate) (PMMA) molecules with various chain numbers has been synthesised using Emulsifier-free emulsion polymerisation method. Langmuir–Blodgett thin film technique is an excellent method to investigate the surface behaviours of organic monolayers at the air–water interface. In this study, PMMA molecules have been studied at the air–water interface using Langmuir–Blodgett thin film method. Area per molecule for several PMMA molecules is found to be between 0.29 ± 0.01 and 0.98 ± 0.01 nm^2. The surface pressure–area graphs were taken in two stages i.e. during the first compression of the monolayer and also during the second compression of the same monolayer before the collapsed stage of the monolayer. It is also found that first surface pressure–area graph for the first compressing of the monolayer at the water surface is different than the surface pressure–area graph obtained after a decompression of the monolayer. Isotherm graphs show that long alkyl chain groups of these molecules may cause aggregation behaviours on water surface and a model for the behaviour of PMMA molecules on the air–water interface due to surface interactions has been proposed.

Keywords: Langmuir–Blodgett films; Monolayers; Surface Pressure; Polymers

1. Introduction

A wide range of polymer materials are synthesised for their potential applications such as light emitting diode [1], conducting polymers [2] and gas sensing applications [3]. Poly(methyl methacrylate) (PMMA) is a transparent, hard and rigid plastic material and it is often used as a shatterproof replacement for glass and a low temperature non-viscous solvent for lubricating oils and hydraulic fluids. The property of optical loss less than 4% due to reflection at the polymer/air interface makes PMMA suitable materials for the cores of communications grade polymer optical fibres and also substrates for polymer optoelectronic devices and integrated waveguides [4]. Low optical loss in the visible spectrum, low lateral shrinkage, high scratch hardness and a glass transition temperature are achieved for PMMA based transparent organic–inorganic hybrid materials by optimising interacting variables acid catalyst concentration, polymer molecular weight, polymer composition and thermal treatment [5].

In order to fabricate a thin polymer film using Langmuir–Blodgett thin film deposition technique [6], it is very important to know the monolayer properties at the air–water interface [7,8]. Most polymer materials including polythiophenes, polyamides [9,10] are shown to form relatively stable polymer monolayers at the air–water interface [11,12].

In this work, the monolayer properties of PMMA molecules with different number of chains are investigated at the air–water interface. The area per molecule for each PMMA molecule is calculated using isotherm graph of each PMMA molecules. After taking the first isotherm graph, the monolayer at the water surface is decompressed to get a second isotherm. Our results show that second isotherm is not identical to the first isotherm. All details will be discussed in the experimental section.

* Corresponding author.
E-mail addresses: ibasaran@balikesir.edu.tr (I. Çapan), rcapan@balikesir.edu.tr (R. Çapan), taner@balikesir.edu.tr (T. Tanrisever), sedacan@balikesir.edu.tr (S. Can).

0167-577X/$ - see front matter © 2005 Elsevier B.V. All rights reserved.
doi:10.1016/j.matlet.2005.03.026

2. Experimental details

A new modified poly(methyl methacrylate) polymer was synthesised with different chain lengths using Emulsifier-Free Emulsion polymerisation method [13] to investigate their monolayer properties at air–water interface. Fig. 1 shows the chemical structure of PMMA molecule and Table 1 summarises all details of PMMA polymers formed at the different temperature. SEM results [13] showed that the size of PMMA beads decreases with increasing temperature due to the increasing decomposition rate of the initiator and increasing monolayer solubility in the aqueous phase on raising temperature, which increase the concentration of growing chains and, thus, reduce the bead size.

All PMMA molecules were dissolved in chloroform with a ratio of concentration around 2 mg ml^{-1}. A computer controlled NIMA 622 LB film trough was employed to investigate the behaviour of PMMA molecules at the air–water interface. The temperature of the water subphase was controlled using Lauda Ecoline RE 204 model temperature control unit and all experimental data were taken at room temperature. Solutions were spread onto the water surface using a microlitre syringe and approximately 15 min were allowed for the chloroform to evaporate. PMMA monolayer at the air–water interface was compressed by moveable barrier with a predetermined barrier speed. Surface pressure was recorded as a function of surface area that is well known as an isotherm graph. All isotherms for PMMA molecules were recorded several times. The area per molecule, a, is calculated using the isotherm graph and can be described by [14]:

$$a = \frac{AM_w}{cN_A V} \quad (1)$$

where A is the enclosed area, M_w is the molecular weight of the material, c is the concentration of the solution, V is the volume of the spread solution onto the water surface and N_A is the Avogadro number.

3. Results and discussion

The movable barriers are employed to enclose an area of the water surface by compressing the PMMA monolayer with a predetermined value of barrier speed. The surface pressure is controlled using a Wilhemly plate method [14]. By compressing the barriers, a plot of surface pressure against surface area can be obtained. After recording first isotherm graph, PMMA monolayer is decompressed again and the second isotherm graph is taken after 5 min. Fig. 2 shows the surface pressure as a function of area per molecule for PMMA-1. Similar results were observed for PMMA-2 and PMMA-3. Phase transition properties for these isotherm graphs are summarised in Table 2. Usually, traditional LB film materials show a very similar isotherm graph even if the monolayer compresses for several times, but in our experiment, the second isotherm is not very similar to the first one. For the first compression displayed in Fig. 2, phase transitions occur at the area per molecule of 1.8, 1.2 and 0.6 nm^2. This isotherm graph has a plateau region around 20 mNm^{-1}. During the second compression, the isotherm also shows phase transitions at the values of 1.1, 0.7 and 0.5 nm^2. Plateau region is completely lost in the second isotherm. Kim et al. [17] studied the molecular conformations of stereoregular PMMA monolayer using scanning probe microscopes (STM and AFM) and suggested that the phase transition is due to the high dipole moment which is constant after a certain surface pressure. Similar phase transitions have been found for stereoregular PMMA monolayer.

Cox et al. [15] studied polystyrene-poly(ethylene oxide) diblock copolymers at the air–water interface and suggested that the reason for the formation of aggregates may be

Table 1
Chemical properties of PMMA molecules

Material	Synthesised temperature (°C)	Particle diameter (mm)	Molecular weight (kg/mol)	Number of units (n)	Purity
PMMA-1	75	0.22	760	18536	98%
PMMA-2	65	0.27	1200	26268	98%
PMMA-3	60	0.28	1100	26829	98%

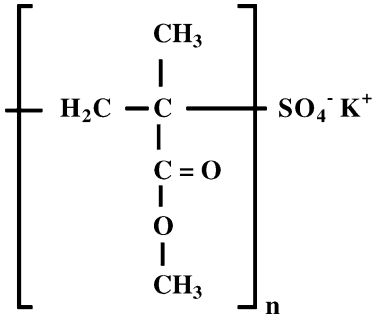

Fig. 1. Chemical structure of PMMA molecules.

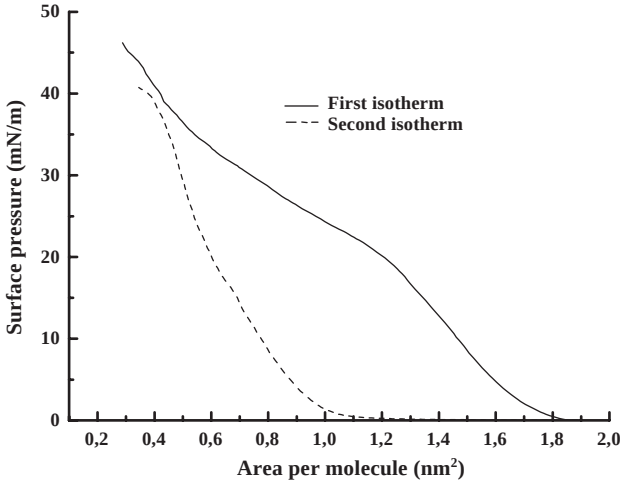

Fig. 2. Isotherm graphs for material PMMA-1.

Table 2
Phase transition regions for isotherms of PMMA molecules

Material	First gas phase (mN m^{-1})	First liquid phase (mN m^{-1})	First solid phase (mN m^{-1})	Second gas phase (mN m^{-1})	Second liquid phase (mN m^{-1})	Second solid phase (mN m^{-1})	Collapse (mN m^{-1})
PMMA-1	~ 0–2	~ 2–8	~ 8–20	~ 20–22	~ 22–28	~ 28–40	≥ 40
PMMA-2	~ 0–1	~ 1–4	~ 4–14	~ 14–17	~ 17–24	~ 24–34	≥ 34
PMMA-3	~ 0–1	~ 1–3	~ 3–14	~ 14–16	~ 16–20	~ 20–30	≥ 30
PMMA-4	~ 0–1	~ 2–26	~ 26–38	–	–	–	≥ 38

started in the solution or on the water surface due to their long tails. The compression of the monolayer could increase the aggregation behaviour. Another work showed that the alkyl chains go into one within the other at the water surface and it is difficult to get back to the initial aggregates [16]. These results suggested us that the reason of the difference between two isotherm graphs could be the long alkyl chains because PMMA molecules (PMMA-1, PMMA-2 and PMMA-3) used in this work have a long tail group.

In order to study the effect of long tail group, a PMMA molecule called PMMA-4 is synthesised with a short chain length (molecular weight: 272 kg mol^{-1}, number of units: 6634, purity: 98%). The same procedure is repeated for PMMA-4 and the isotherm obtained during the second compression occupies less area per molecule than the isotherm obtained during the first compression for PMMA-4 as shown in Fig. 3. It can also be explained by the fact that the PMMA is no longer forming a monolayer after the second compression. Some of the molecules override to the top of the first monolayer forming double or more monolayer. A representative model for the formation of this aggregate is shown in Fig. 4. When the molecules are in gas phase shown in Fig. 4a, the interaction between molecules is very small and a few aggregates could be formed. When the barriers are closed very gently, molecules get closer and the interaction between molecules increases. It is known as the liquid phase given in Fig. 4b. In the solid phase (see Fig. 4c), the aggregates of molecules get closer so that the surface pressure dramatically increases. Further compression makes the monolayer to a more complex structure as shown in Fig. 4d.

Isotherm graphs and Eq. (1) are used to calculate the area per molecule for PMMA monolayer at the selected surface pressure values. Fig. 5 shows area per molecule as a function of number of chains. The molecular area is

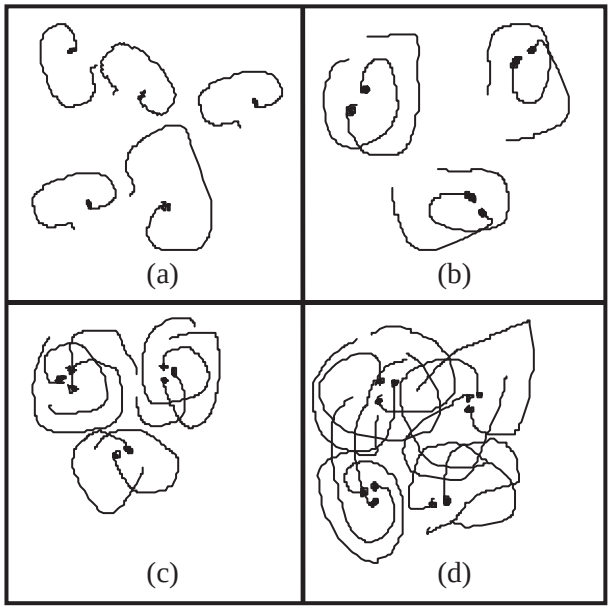

Fig. 4. Representative model for the formation of aggregates on water surface (a) gas phase, (b) liquid phase, (c) solid phase and (d) collapse.

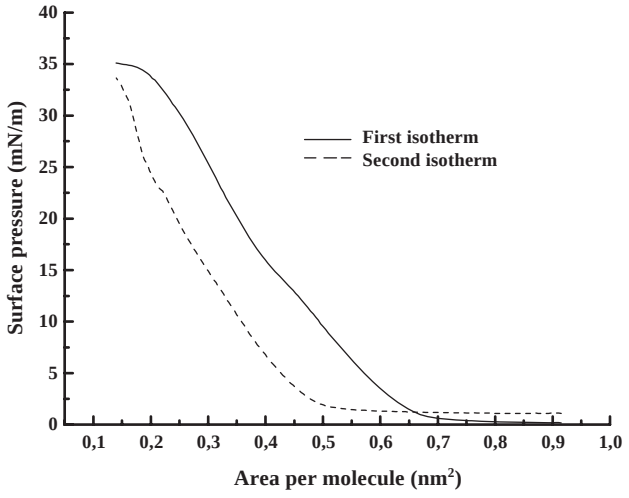

Fig. 3. Isotherm graphs for material PMMA-4.

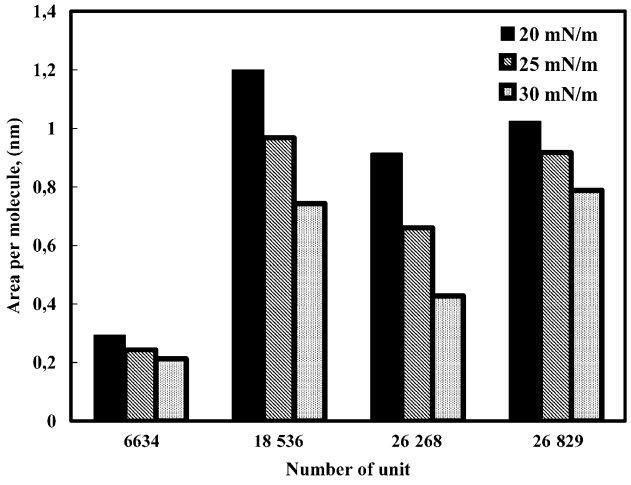

Fig. 5. Area per molecule for PMMA materials at different surface pressures.

increasing with the increasing chain number so that PMMA molecules with a long chain occupy bigger surface area than PMMA molecules with a short chain. The alignment of the chain could make a circular conformation around the head group. This could be that the molecule is not perpendicular to the water surface.

4. Conclusion

PMMA molecules with different number of chains are fabricated to investigate the monolayer properties at the air–water interface using Langmuir–Blodgett thin film technique. Isotherm graphs at the air–water interface are recorded for each PMMA molecule. Area per molecule for these molecules is found to be between 0.29 ± 0.01 and 0.98 ± 0.01 nm^2. The investigation does show that the length of alkyl chain does influence the isotherm of the PMMA polymer only if we compare PMMA-4 with PMMA-1 or PMMA-2 and PMMA-3. However, if we compare isotherm for PMMA-1 with PMMA-2 and PMMA-3, the results show that the isotherms are similar even though PMMA-2 is longer than PMMA-1 and PMMA-3 is also than PMMA-1. Our future work will be focused on Brewster Angle Microscopy, Atomic Force Microscopy and Ellipsometry measurements for a deep investigation of the change of isotherm graphs. Another target is to fabricate an LB film gas sensor device using these PMMA molecules.

References

[1] J.H. Burroughes, D.D.C. Bradley, A.R. Brown, R.N. Marks, K. Mackay, R.H. Friend, P.L. Burns, A.B. Holmes, Nature 347 (1990) 539.
[2] Z. Liang, M. Rackaitis, K. Li, E. Manias, Q. Wang, Chem. Matters 15 (2003) 2699.
[3] R. Capan, A.K. Ray, A.K. Hassan, T. Tanrisever, J. Phys., D. Appl. Phys. 36 (2003) 1115.
[4] A. Zoubir, C. Lopez, M. Richardson, K. Richardson, Opt. Lett. 29 (16) (2004) 1840–1842.
[5] J.H. Harreld, A. Esaki, G.D. Stucky, Chem. Mater. 15 (18) (2003) 3481–3489.
[6] A. Ulman, An Introduction to Ultrathin Organic Films, Academic Press Inc., New York, 1991.
[7] J. Zhu, A. Eisenberg, R.B. Lennox, J. Am. Chem. Soc. 113 (1991) 5583.
[8] J. Zhu, A. Eisenberg, R.B. Lennox, Makromol. Chem. 53 (1992) 211.
[9] F.R. Ahmed, E.G. Wilson, G.P. Moss, Thin Solids Films 187 (1990) 141.
[10] G.L. Gaines, Langmuir 7 (1991) 834.
[11] K.U. Fulda, B. Tieke, Supramol. Sci. 4 (1997) 265.
[12] R. Heger, W.A. Goedel, Supramol. Sci. 4 (1997) 301.
[13] T. Tanrisever, O. Okay, Y.Ç. Sönmezoglu, J. Appl. Polym. Sci. 61 (1996) 485.
[14] M.C. Petty, Langmuir–Blodgett Films, Chambridge University Press, 1996.
[15] J.K. Cox, K. Yu, B. Constantine, A. Eisenberg, R.B. Lennox, Langmuir 15 (1999) 7714.
[16] Y. Seo, J.-H. Im, J.-S. Lee, J.-H. Kim, Macromolecules 34 (2001) 4842.
[17] J.J. Kim, S.D. Jung, W.Y. Hwang, ETRI J. 18 (1996) 195.